Korean J. Chem. Eng., 40(4), 770-790 (2023)
DOI: 10.1007/s11814-022-1342-6

pISSN: 0256-1115
eISSN: 1975-7220

The influence of different twisted tape inserts configurations on thermo-hydraulic performance and enhancement of heat transfer in the 3D circular tube

Ahmed Ramadhan Al-Obaidi†

Mustansiriyah University, College of Engineering, Mechanical Engineering Department, Baghdad, Iraq
(*Received 2 April 2022 • Revised 9 September 2022 • Accepted 6 November 2022*)

Abstract−Numerical simulation was performed to analyze the behavior of a flow field, characteristic of pressure drop, and hydraulic thermal performance. Moreover, influences of different twisted tape geometric parameters, including three twisted tape inserts (NTTI) 1, 3 and 5. Also, six different twisted turns (NTT) were comparably quantitative and qualitative studied using various important parameters, including static pressure, dynamic pressure, and velocity magnitude, respectively. The results revealed that the value of pressure drop between each cross section in the pipe decreases as pipe length increases. When the NTTIs increases that leads to a pressure difference also increasing as compared to the smooth pipe. It is found that inserting twisted tape in the pipe leads causes considerably high resistance in the flow, then leads to increase the pressure difference. In addition, the results show that existence of the twisted tapes inside the pipe can create more vortex motion (swirl flows) that leads to formation of different radial velocities. Also, the PEF factor decreases as the Re increases. The comparison results for the numerical and experimental indicate that a good agreement of the average deviation for f (friction factor) and Nu is around 6.5% and 7%. The minimum Nu number value was 10 for NTT1 at Re number of 900 and the higher value was 50 at Re of 14,000. The PEF is more than 1.6 for NTT6 configuration. The results indicate that the temperature difference increases up to 38.1%, 46.11% and 50.52% with increasing the NTTI from 1 to 5, respectively, as compared to the temperature difference in a smooth pipe.

Keywords: Twisted Tape Inserts, Fluid Flow Characteristics, Pressure Drop, Thermo-hydraulic Performance, Heat Transfer Enhancement, CFD Method

INTRODUCTION

The augmentation of heat transfer systems is frequently used in different areas in industrial and domestic applications, such as in air-conditioning equipment, thermal power plants, cooling and heating systems [1]. The techniques of passive and active are commonly used in the heat transfer augmentation [2]. The most important effective method to enhance the passive heat transfer technology is twisted tape insert [3,4]. Commonly, the most passive methods are generating mixing and an increasing surface area. Using the latter methods can effectively enhance the transfer coefficient [5,6]. Generating perturbation inside the circular using tape insert or twisting a pipe wall can improve the heat transfer in the pipes of a heat exchanger [7-10]. Twisted tapes are the vital enhancement of passive heat transfer technology due providing more energy saving and there is no need to input extra energy. Also, twisted tapes are frequently designed to reduce volume size as well as decrease initial construction cost of heat exchangers and promotion of existing heat exchangers for retrofit, because they have low cost, easy fabrication, and convenient assembly. Twisted tapes are gaining increasing interest because they play a vital role in energy saving and conversion. Different research has been carried out in the designs of twisted tape in order to increase the rate of heat transfer rate, but this work still needs more improvement. Salman et al. [11] analyzed numerically the characteristics of thermal behavior in a circular pipe using twisted tape type horizontal baffles. Twisted tape is the important shape used to enhance the heat transfer in various heat exchanger applications. Results have shown that decreasing the twist ratio (Length of one twist/twist diameter) can enhance the Nusselt number when the Reynolds number increases. Also, they found that a twisted tape ratio equal y=2.93 can provide high heat transfer enhancement.

Another numerical investigation was carried out Erdemir by et al. [12] to enhance the heat transfer and pressure drop using dual twisted tape. They found that the use of that type of twisted tape can significantly increase the pressure drop and heat transfer in pipes. Also, results indicate that the maximum enhancement efficiency was around 27% under a Reynolds number nearly to 3920. Varma et al. [13] enhanced the heat transfer using cut twisted tape inserts by applying CFD analysis method. They observed that from velocity contours at different cross-sectional areas the eddy flow can produce more vortex than that causing more formation of turbulent flow due to inserting the twisted tapes. Hence, there was a significant rise in coefficient of heat transfer and Nusselt number. Mashoofi et al. [14] studied the influence of axially inserting tapes on the enhancement of thermal performance in heat exchanger double pipe. The results showed that using this type of twisted tape could importantly increase the thermal performance as compared to without twisted tape. Hosseinnejad et al. [15] studied adding the twisted inserting tape on the turbulent heat in tubular pipes of a heat exchanger. Numerical results indicated that two types of distinct rotational areas took place. Moreover, more large rotational areas at aligned orientation have been observed in the pipe due to inserting

†To whom correspondence should be addressed.
E-mail: ahmedram@uomustansiriyah.edu.iq

the twisted tape.

Furthermore, as torsion ratio decreased, the Nusselt number increased at high Reynolds numbers. Saravanana et al. [16] studied the forced flow and augmentation of heat transfer in a solar collector using square and V-cut cut tapes twisted. They found that using this type of twisted tape can enhance the rate of heat transfer about 8.86% as compared to the collector type flat plate. Alzahrani et al. [17] analyzed the influence of twisted tape design on thermal performance and pressure loss in circular pipe. It was found that as the (pitch over diameter) twist ratio decreased the pressure drop and heat transfer coefficient increased by 102.8% and 28%. Moreover, at the smallest twist ratio the maximum pressure drop and heat transfer enhancement can be found. Furthermore, as the tape width decreased, both pressure drop and heat transfer enhancement also decreased. Xi et al. [18] investigated using angular twisted square wire to enhance the heat transfer. The results revealed that using this type can improve the heat transfer rate as compered without twisted. Nakhchi and Esfahani [19] numerically analyzed the effect of using cross-cut twisted tape in heat exchanger pipes. They found that when the twisted tape width to diameter ratio increased, that led to heat transfer also increased. Moreover, the results indicated that using twisted tape can significantly affect the rate of heat transfer, especially at low range of flow rates. Liang et al. [20] conducted heat performance in the laminar flow behavior using inserting a center tapered wavy tape in the pipe. The results observed were that this type of twisted tape has important effect on decreasing the resistance of flow and improving heat performance. The results found that increasing the Nusselt number between 5.23 to 8.99 times also increased the performance evaluation criterion to 2.62 times. Hong et al. [21] conducted the fluid flow characteristics and turbulent thermal within a plain pipe with different twisted tapes. The outcomes display that the values of both f and Nu increase as tape number increases and decline with ratio of overlapped twisted. Experimental outcomes prove the increase in tape number and reducing overlapped twisted ratio caused by the decrease of the value of entropy generation owing to heat transfer rate as well as the increase of entropy generation owing to increase friction resistance.

Later Kumar et al. [22] studied the heat characteristics inside the circular pipe through the use of multiple twisted tapes under conditions of laminar flow. It was shown that two tapes insertion can increase the heat performance in a circular pipe when compared to the single tape insertion in terms of a Nu number and higher friction factor. Also, results noted that the swirl condition at the value of Re of 1,000 the values of Nu and friction factor were higher than the single tape by 38% and 29%, respectively. Moreover, counter-swirl increased the Nu and friction factor by 43% and 34% as compared to single tape. Piriyarungrod et al. [23] intensified heat performance within a heat exchanger pipe using multiple twisted inserts. It was found that thermo-hydraulic performance, friction factor and Nu increased with multiple twisted tapes increasing. Safikhani et al. [24] studied using nanofluid flow in pipes by using multiple twisted tapes. The obtained outcomes show that using two twisted tapes insertion in varying flow directions increases both pressure and heat transfer in pipes. The rise in friction factor and heat performance in pipes was more than 220% and 50%, respectively. Ghalambaz et al., Arasteh et al., Mashayekhi Arasteh et al., and Miandoab et al. [25-31] studied the effect of different twisted tape insert geometrical configurations. They noted that using these types can impact the thermal performance in the heat exchanger pipes and then increase the overall thermal performance in the system.

Though, the above studies still did not cover the available enhancement approaches. Particularly, numerical techniques need more investigations for enhancement of heat transfer rate. Computational numerical simulation technique has different beneficial advantageous to predict the performance connected to the increase of heat performance using the insert of twisted tape to explain the mechanisms of fluid flow, thermo-hydraulic and heat performance in the heat exchanger pipes. Therefore, in the current study, a numerical investigation of flow, thermo-hydraulic performance, pressure loss, and enhancement of thermal performance in three-dimensional tube with and without twisted tape insert at different geometrical configurations was carried out using CFD technique. The important goal of this investigation is to predict the flow field behavior, thermo-hydraulic flow and heat transfer characteristics along the pipe and at different cross sections. The qualitative and quantitative results are presented as static pressure, dynamic pressure, different velocities, temperature, turbulent kinetic energy and wall shear stress, friction factor, Nu number and ratios of f/fo and Nu/Nuo.

PHYSICAL MODEL WITH AND WITHOUT TWISTED TAPE INSERT

Fig. 1 represents three dimensional geometrical configuration of several enhanced pipes. To enhance the performance of heat transfer, a designed physical model including 1920mm pipe fluid domain and 10.80 mm diameter were inserted different number of twisted tapes, namely, 1, 3 and 5 and at six twisted turns (NTT). As shown in this figure, all these twisted tapes have thickness of 1 mm and width of 2mm. All flow domain for pipe and twisted tape insert is modelled using CFD methods. The water properties employed for numerical simulation are summarized in Table 1. Also, the computational flow domain schematic for (a) Smooth pipe and (b) twist tape insert is in Fig. 2.

1. Mathematical Model Details

In this work, the implementation of temperature profiles and fully developed flow by recompilation and assuming the properties of pure fluid thermophysical are constant. The mass conservation, momentum, and energy equations are to be encountered. By applying the above assumptions, the governing equations can be written as follows:

Table 1. The properties of water [3]

Properties	Parameter	Value of properties	Unit of properties
Thermal conductivity	k	0.63	W/m·K
Dynamic viscosity	μ	6.71E-04	N·s/m^2
Specific water heat	C_p	4178	J/kg·K
Density of water	ρ	992.32	kg/m^3

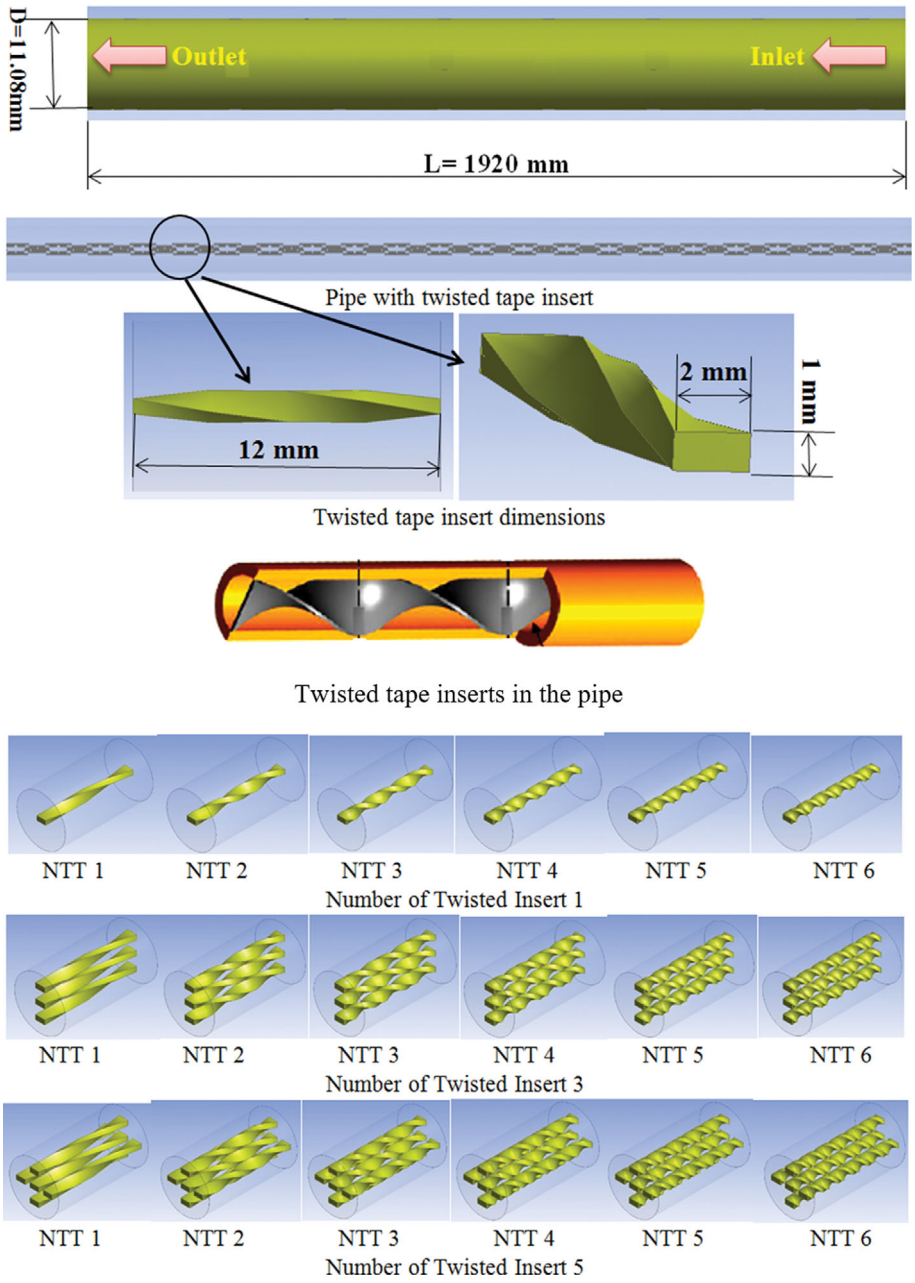

Fig. 1. Schematic diagram of the three dimension flow domain for the pipe and different twisted tape inserts.

1-1. Continuity Equation [3]:

$$\frac{\partial}{\partial x_i}(\rho u_i)=0 \tag{1}$$

$$\frac{\partial u}{\partial x}+\frac{\partial v}{\partial y}+\frac{\partial w}{\partial z}=0 \tag{2}$$

Momentum equation [3]:

Using Newton's second law of motion the momentum equations for differential fluid volume can be derived [3].

$$\frac{\partial(\rho u_i u_j)}{\partial x_j}=-\frac{\partial p}{\partial x_i}+\frac{\partial}{\partial x_j}\left[\mu\left(\frac{\partial u_i}{\partial x_j}+\frac{\partial u_j}{\partial x_i}\right)\right]-\frac{2}{3}\delta_{ij}\frac{\partial u_k}{\partial x_k} \tag{3}$$

Energy equation [32]:

$$\frac{\partial}{\partial x_j}(u_i(\rho E+p))=\frac{\partial}{\partial x_j}\left[\left(\lambda+\frac{C_p\mu_t}{Pr_t}\right)-\frac{\partial T}{\partial x_j}+u_i(\tau_{ij})_{eff}\right] \tag{4}$$

The E represents total energy and the term $(\tau_{ij})_{eff}$ denotes a stress tensor deviated expressed as follows:

$$E=C_pT-\left(\frac{p}{\rho}\right)+\frac{u^2}{2} \tag{5}$$

$$(\tau_{ij})_{eff}=\left[\mu_{eff}\left(\frac{\partial u_j}{\partial x_i}+\frac{\partial u_i}{\partial x_j}\right)-\frac{2}{3}\mu_{eff}\frac{\partial u_i}{\partial x_j}\delta_{ij}\right] \tag{6}$$

The equations of turbulent kinetic energy and turbulent frequency

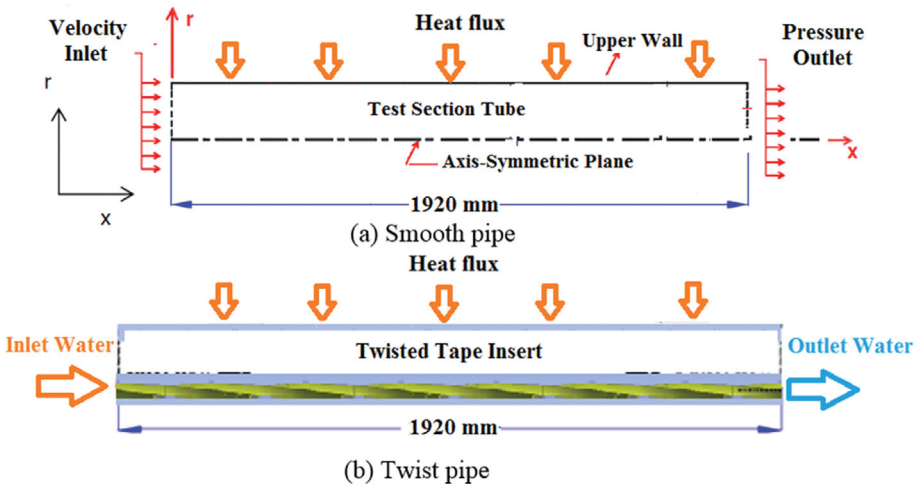

Fig. 2. The computational flow domain schematic for (a) Smooth pipe and (b) Twist tape insert.

have been calculated as follows:

$$\frac{\partial}{\partial x_i}(k u_i) = -\frac{1}{\rho}\left(\frac{\partial}{\partial x_j}\left(\Gamma_k \frac{\partial k}{\partial x_j}\right) + \widetilde{G_k} - Y_k + S_k\right) \quad (7)$$

$$\frac{\partial}{\partial x_j}(\rho\omega u_j) = \frac{1}{\rho}\left(\frac{\partial}{\partial x_j}\left(\Gamma_\omega \frac{\partial \omega}{\partial x_j}\right) + G_\omega - Y_\omega + D_\omega + S_\omega\right) \quad (8)$$

The G_k represents turbulent kinetic energy generation owing to the average of velocity gradients, G_ω denotes the generation frequency (ω), S represents the source term for ω and k, Y_k is the dissipation due to the turbulence for ω and k.

In the current numerical study, the turbulence model K–ε (RNG) is adopted [32].

The friction factor (f) for the characteristics of fluid flow can be estimated as [32]:

$$f = \frac{\Delta P}{(\rho u^2/2)(L/d_i)} \quad (9)$$

As seen from above equation, the friction factor is highly affected by the pressure difference across the pipe at inlet and outlet.

According to the properties of thermo-physical working fluid for velocity, viscosity, density and inner tube diameter the Re can be calculated as [32]:

$$Re = \frac{\rho u D_i}{\mu} \quad (10)$$

where D_i, u, and are the inner diameter, velocity and density of the

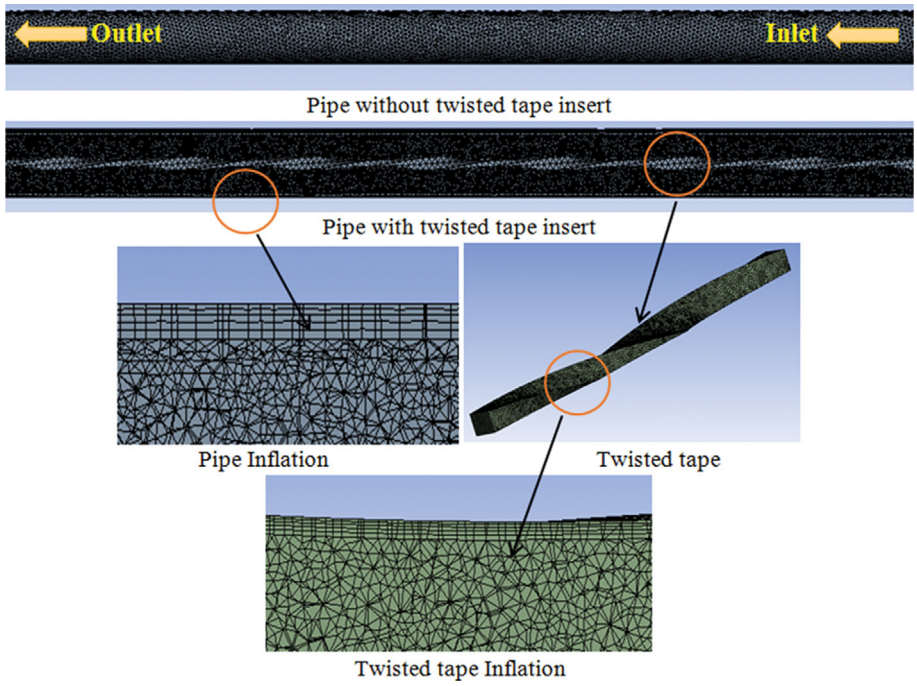

Fig. 3. Three dimension schematic of meshing flow domain for normal pipe and pipe with insert twisted tape.

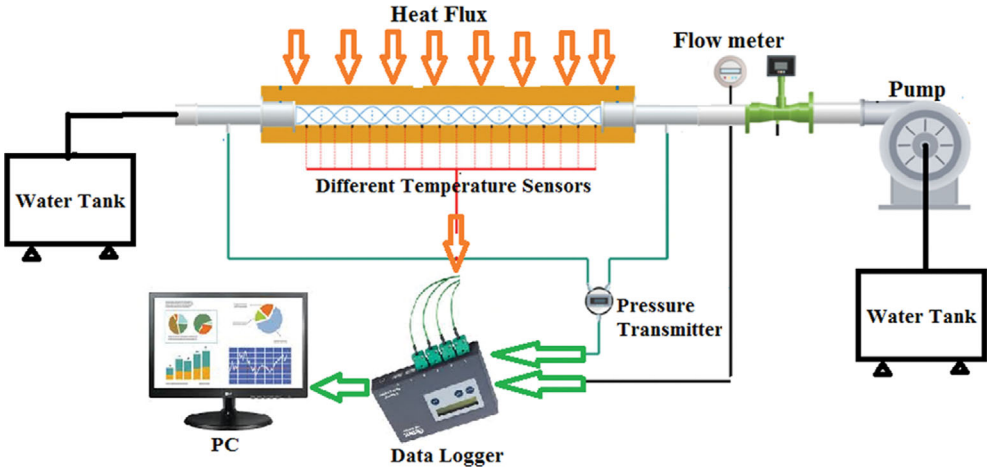

Fig. 4. Experimental test rig schematic diagram.

water [33].

The heat transfer in the pipe can be calculated using Eq. (11):

$$Q=m\,C_p\,\Delta T \tag{11}$$

The equation of Nusselt number can be written as follows:

$$N_u=\frac{h_f D_e}{k_f} \tag{12}$$

The evaluation criterion (PEF) can be calculated as follows:

$$PEF=\frac{N_u/N_{u_0}}{(f/f_0)^{1/3}} \tag{13}$$

2. Boundary Conditions

The boundary conditions are velocity inlet at inlet and pressure outlet condition at the outlet. In the system at inlet the mass weighted average of pressure provides the pressure drop. Numerical calculations are modelled for both with and without twisted tape insert at constant coefficient of heat flux 800 W/m^2. The Navier-Stokes equations connected with energy equation are solved.

$$\text{The velocity at the inlet: } U_m=U_i \tag{14}$$

Mean velocity in the pipe wit Reynolds number in circular tube can be shown as the following equation:

$$Um=4m/\pi\rho Di \tag{15}$$

3. Convergence Criteria and Solution Numerical Methods

In this numerical simulation, the semi-implicit pressure linked correlation (SIMPLE) was employed for coupling the pressure and velocity technique. Steady state conditions and gravity independence were carried out. For continuity, momentum and energy equations the 2nd order of up winding was chosen to exam the different variables within every cell. Computational solutions were performed until the energy and continuity residue reached to 10^{-6}.

4. Meshing the Flow Domain

The mesh of the pipe with and without twisted tape insert with inflation layers at the boundary was carried out using the ANSYS Workbench as shown in Fig. 3. The mesh flow is checked under different mesh independent tests in order to obtain good accu-

Table 2. Study of the grid test independency

Grids (million)	Nu (-)	Difference (%)
1.43	58.50	
2.65	60.81	3.76
3.65	62.32	2.41

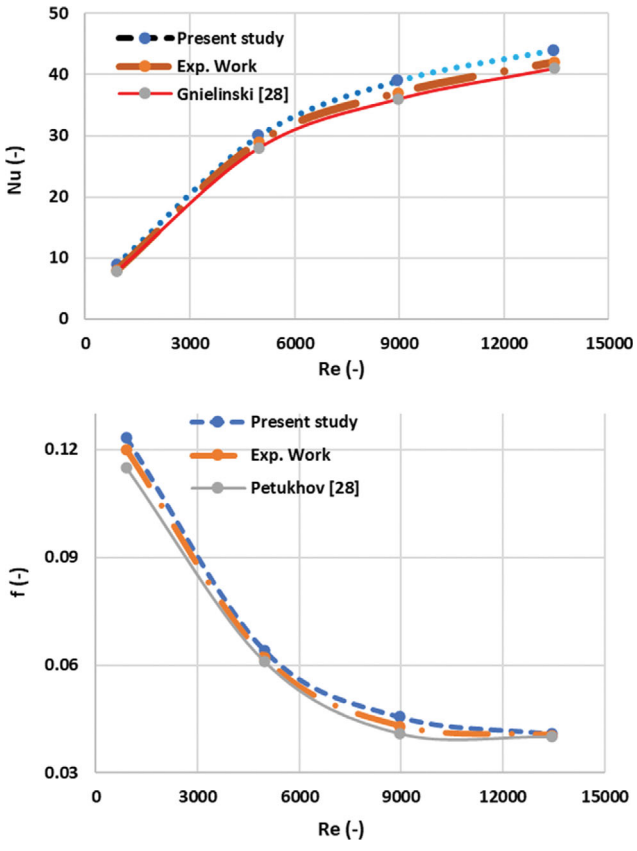

Fig. 5. Experimental, numerical and correlations validation results.

racy results; the total number of mesh elements tests was one, two and three million, respectively. The grid tests were analyzed using pressure differences at inlet and outlet of the pipe at conditions including rate of flow 0.56 l/min, temperature 313 K and heat flux 800 W/m^2. The mesh of three million elements was selected for analyses purposes in this investigation. Varying of mesh grid numbers comprising 1.43, 2.65, and 3.65 million grids of 3.65 million elements was used for analysis purposes because it offers good outcomes as compared to other results as listed in Table 2.

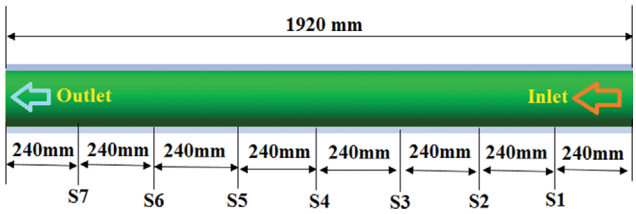

Fig. 6. Divided both smooth and twisted insert pipes to different cross section areas.

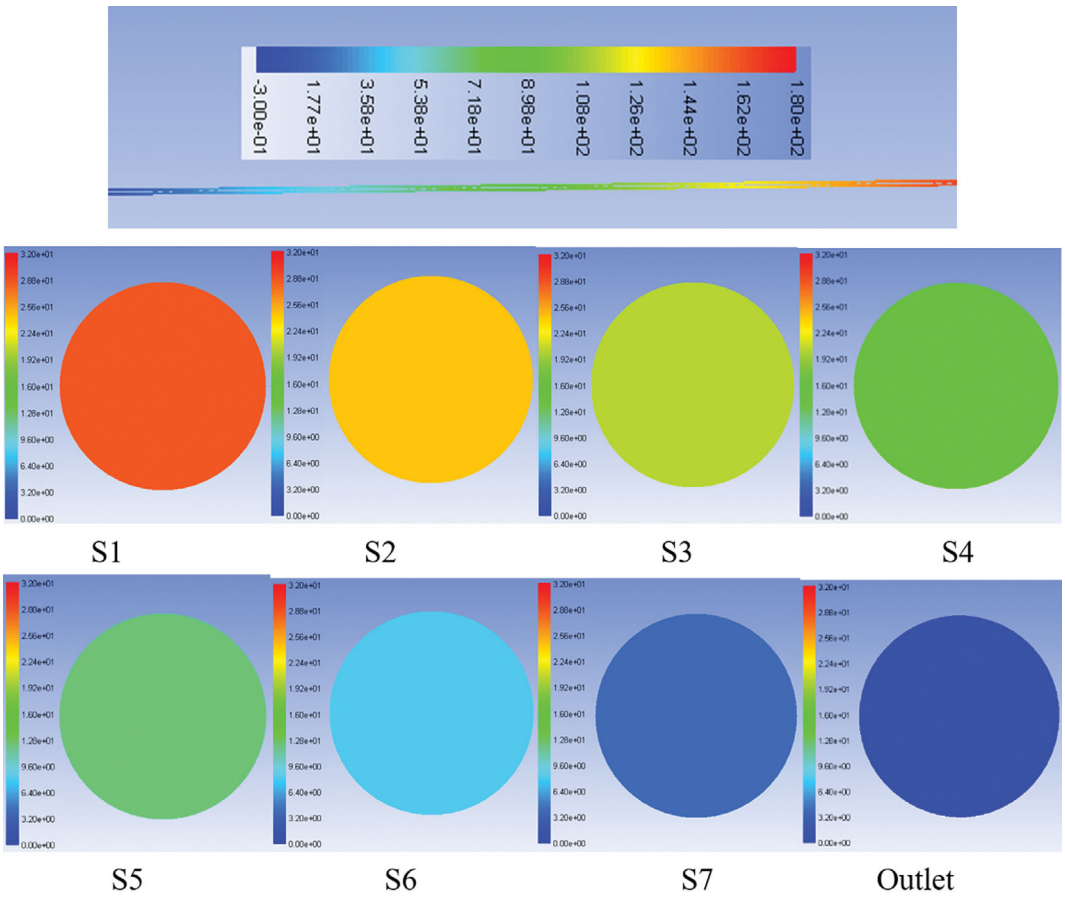

(a) Static pressure variations contour in smooth pipe at different cross sections

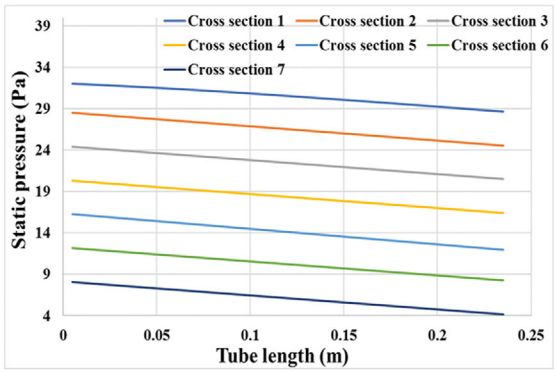

(b) Static pressure drop in smooth pipe at different cross sections

Fig. 7. (a) Static pressure variations contour, and (b) Static pressure drop between each two cross sections in smooth pipe.

FACILITY OF AVAILABLE EXPERIMENTAL TEST

In this study, the numerical results are validated with available experimental results which were carried out by Albanesi [27]. The schematic of experimental rig is depicted in Fig. 4. This test rig includes a pump, test pipe (1,920 mm length and 11.08 mm diameter), pressure transducers to calculate the pressure at inlet and outer, different thermocouples to measure the temperatures at various locations in the pipe, an electrical power supply, data logger and PC.

We used CFD technique to study the improvement of thermal performance in pipes by using twisted tape insert, then investigated the characteristics of fluid flow structure and thermal performance as a significant tool to minimize and provide good accuracy close to experimental data. Therefore, in this work CFD analyses is carried out for a variety of insert tape configurations as presented in the next section.

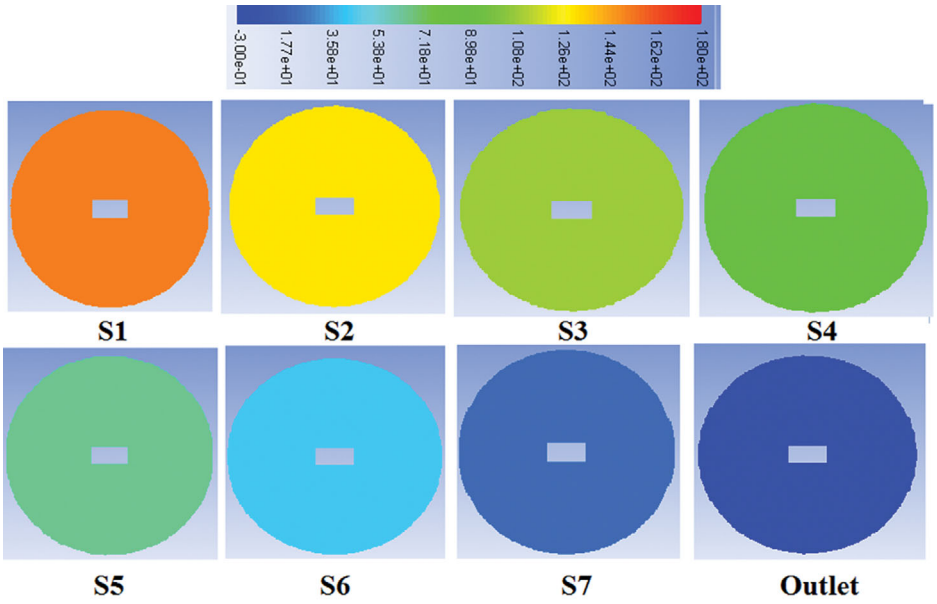

(a) Static pressure variations contour in pipe at different sections

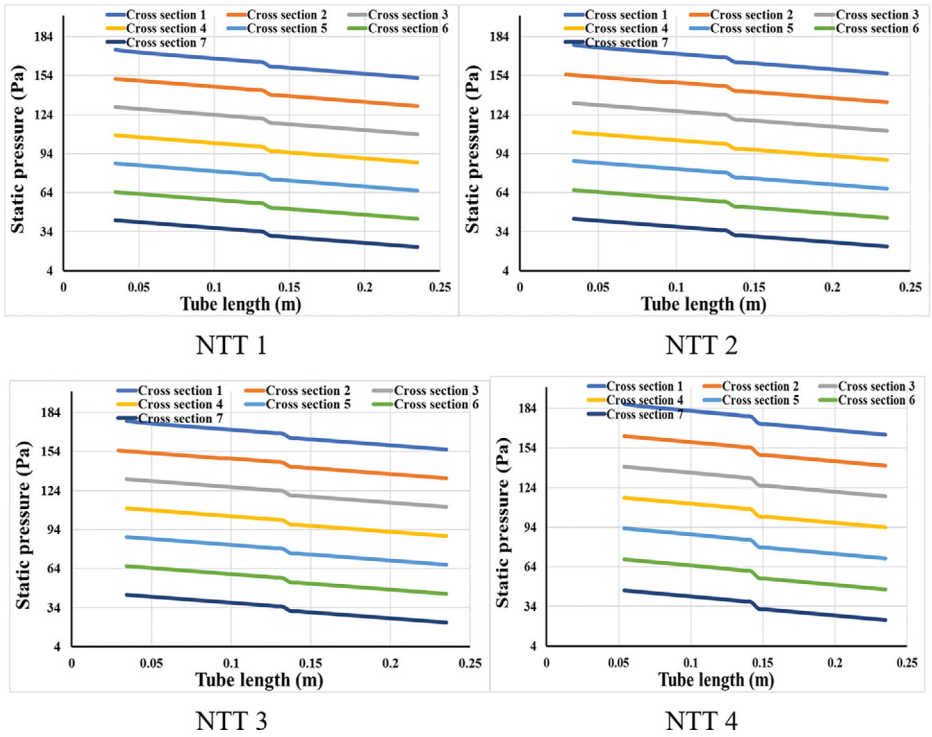

Fig. 8. (a) Static pressure variations contour and (b) Static pressure drop between each two sections in pipe, (c) Nu number validation with previous experimental data.

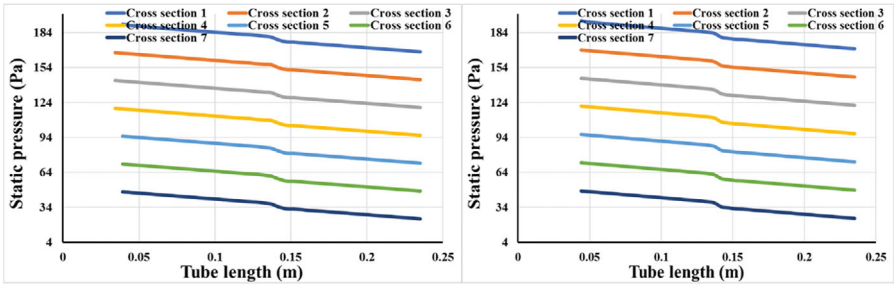

(b)

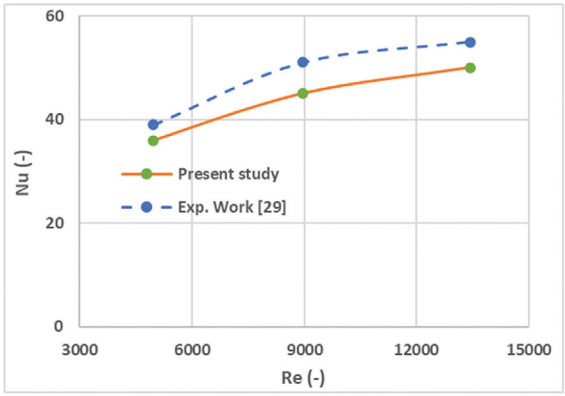

(c)

Fig. 8. Continued.

RESULTS AND DISCUSSION

1. Validation Results

Before studying the heat and thermal-hydraulic performances with varying twisted tape devices, the computational model was validated with available experimental outcomes and with some correlations as represented in Eqs. (16) and (17). Where the Nu and f were the Nusselt number Nu and friction factor f in improved pipes,

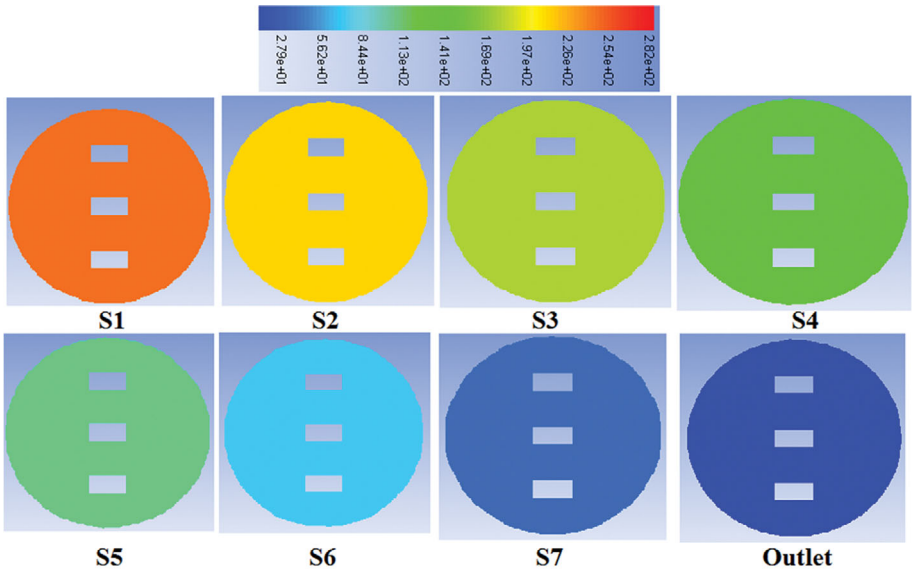

(a) Static pressure variations contour in pipe with three twisted tape insert

Fig. 9. (a) Static pressure variations contour and (b) Static pressure drop between each two cross sections in pipe with three twisted tape inserts.

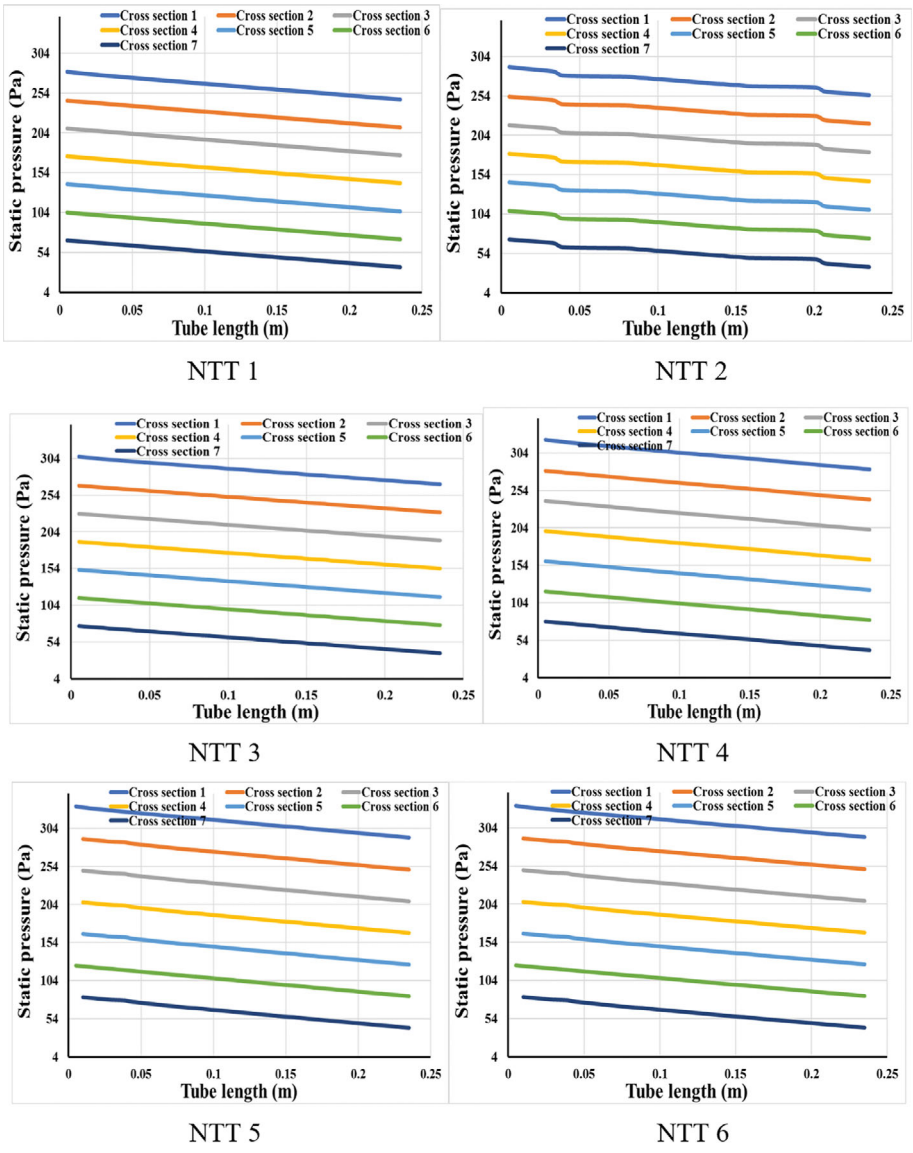

(b) Drop in static pressure at pipe with three tape inserts at variety of sections and various of NTT

Fig. 9. Continued.

whereas the values of f_p and Nu_p are corresponding to the smooth pipe. These values were, respectively, calculated by Petukhov and Gnielinski correlations [35].

The Petukhov Correlation [35]:

$$f_p=(0.79\ln Re-1.64)^{-2} \quad (16)$$

The Gnielinski Correlation:

$$Nu_p=\frac{(f/8)(Re-1{,}000)Pr}{1+12.7(f/8)^{1/2}(Pr^{2/3}-1)} \quad (17)$$

In the present investigation, the turbulent flow with and without twisted tape insert was simulated under Reynolds number ranges between 3,000 and 15,000 in a heat exchanger pipe. In the first step to ensure the precision of the obtained results, the numerical results must be validated with available experimental data as carried out by Albanesi et al. [35]. The comparison between the numerical and experimental results indicates that a good agreement the average deviation between them for f and Nu is around 6.5% and 7%. The outcomes revealed that the numerical results are consistent with the experimental data as shown in Fig. 5. Whereas the error deviations by using Eqs. (16) and (17), reported by Petukhov and Gnielinski [36], are around ±8.5%. According to these outcomes, it can be noted that the numerical model methods are reliable and reasonable.

In the present study, the length of both smooth and twisted tubes was divided into seven cross section areas and they are called S1, S2, S3, S4, S5, S6 and S7 as illustrated in Fig. 6. Each distance between every two cross sections is constant, equal to 240 mm.

2. Analysis the Flow Field Structures Variations

To show the influence of the different twisted tape inserts, the hydraulic and thermal performances in pipes of heat exchanger

were compared with the smooth pipe under the same operating conditions and range of Reynolds number. The first numerical prediction results in this work are depicted in terms of static pressure variations as shown in Fig. 7(a) under conditions including flow rate 0.56 l/min, inlet temperature of 313.15 K and the convective coefficient of heat transfer of 800 W/m^{2}K. The current numerical data demonstrate the static pressure in a smooth pipe gradually decreases as pipe length increases. It can be seen that the maximum pressure takes place at the inlet pipe as shown in section S1. Also, the low value of pressure happens near the end pipe. From Fig. 7(b) it is clearly realized that the pressure drop decreases between every two cross sections in the smooth pipe. Moreover, the minimum value of pressure takes place at section S7.

To investigate thermo-hydraulic performance mechanism due to inserting the different twisted tape configurations, the flow field and temperature variations in the pipe are analyzed.

3. Effects of Twisted Tapes on Flow Field Behavior

Fig. 8(a) represents the static pressure variation in a twisted pipe with various twisted tape inserts, namely 1, 3 and 5, respectively, under the same above operation conditions. It can be observed that the overall all behavior of the static pressure variations in these figures has the same trend in Fig. 9. That means the pressure in a pipe with and without tape insert decreases as the pipe length increases for all cases under investigation. Moreover, the behaviour of the pressure drop in Fig. 8(b) also has the same trend in Fig. 9(b). But the value of pressure in the twisted pipe is more than the normal pipe because inserting the twisted tape inside the pipe can cause more fluid resistance. Furthermore, outcomes revealed that when the twisted tape number (NTTI) increases, a pressure difference in pipe also increases as summarized in Table 2. Fig. 8(b) illustrates static pressure drop in the twisted pipe at different cross sections. According to this figure, all behavior of a static pressure drop is

Table 3. Pressure difference (ΔP) with and without different twisted tape inserts

Smooth pipe	NTT 1	NTT 2	NTT 3	NTT 4	NTT 5	NTT 6
Pressure	Pressure	Pressure	Pressure	Pressure	Pressure	Pressure
Pa	Pa	Pa	Pa	Pa	Pa	Pa
			NTTI 1			
32.05	174.71	179.71	182.59	188.34	192.27	195.10
			NTTI 3			
32.05	281.77	292.01	307.94	323.04	334.50	344.36
			NTTI 5			
32.05	455.82	482.62	525.73	570.36	601.67	633.72

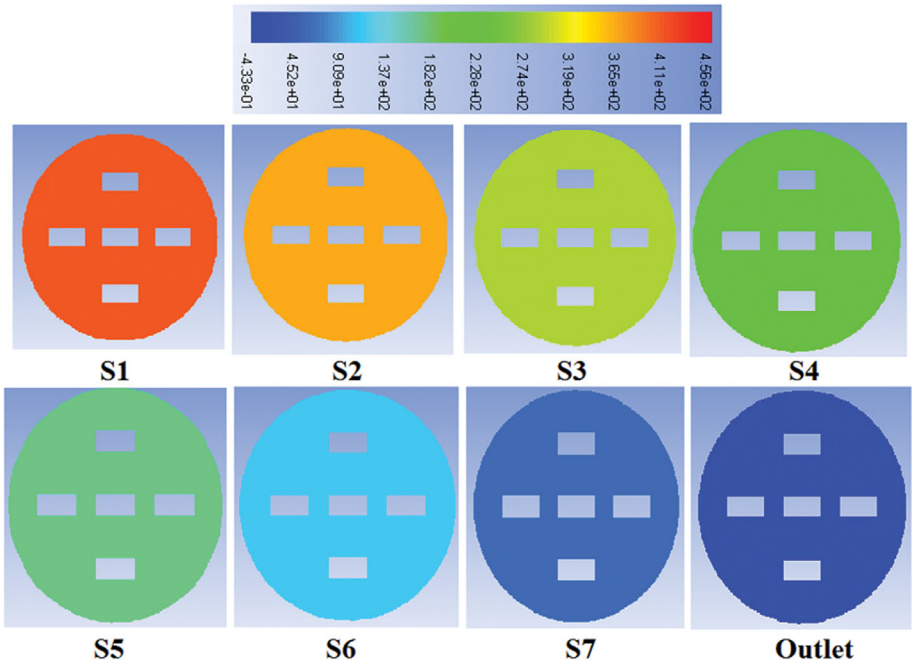

(a) Static pressure variations contour in pipe with five tape inserts

Fig. 10. (a) Static pressure variations contour and (b) Static pressure drop between each two sections.

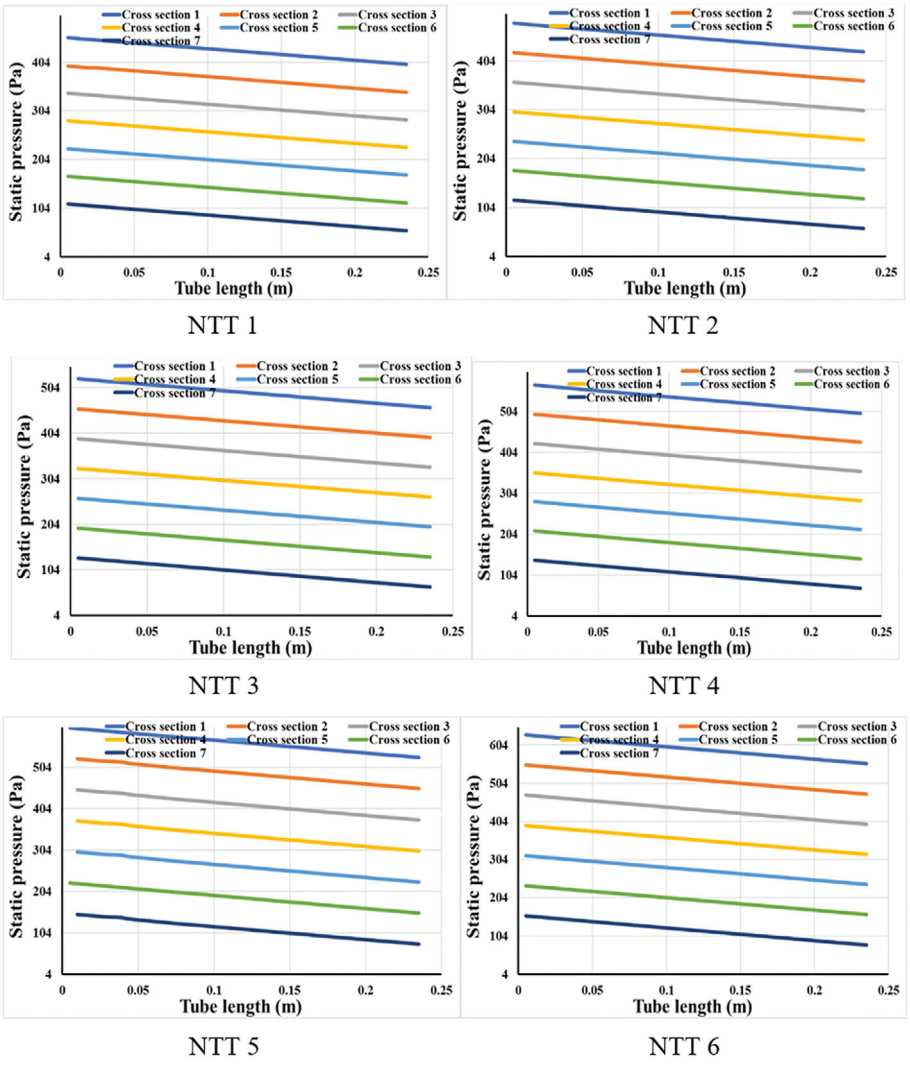

(b) Drop in static pressure at pipe with five tape inserts at various sections and various of NTT

Fig. 10. Continued.

rather similar to pressure drop in Fig. 8(b) but at different value of pressure losses. Moreover, the value of the pressure drop between each cross section in the pipe decreases as pipe length increases for all cases under investigation. Fig. 8(c) illustrates the validation numerical work with experimental data carried out by Hong et al. [29]. It can be noticed that both Nu curves have the same trend, the value of Nu increases as the NTT increases.

The advantage of using the twisted tape is illustrated, but it can cause disadvantages; therefore it should be evaluated. Table 3 summarizes the pressure difference at different NTTIs and NTT. It can be seen that as the NTTIs increases that leads to the pressure difference also increasing as compared to the smooth pipe. It is obvious from this table that using twisted tape in a pipe can lead to considerably highly resistance in the flow, which then leads to increasing the pressure difference. Also, the NTTI has a large effect on the pressure difference. Moreover, the results have shown that NTT has small effect on the value of pressure difference as shown in Fig. 10.

The numerical simulation results can capture the flow structure of the flow files such as dynamic pressure. Fig. 11 illustrates both axial and radial cross sections in the smooth pipe for the dynamic pressure variations at conditions of flow rate 0.56 l/min, inlet temperature of 313.15 K and the coefficient of heat transfer convective of 800 W/m^{2}K. It can be obviously seen that high dynamic pressure happens at the core of the pipe; also, it reaches to the maximum value of the dynamic pressure close to the outlet pipe.

Fig. 12(a) describes the dynamic pressure variation contours of water flow within the circular pipe with TTNI 1 at different NTT. The numerical results revealed that when fixed, the Reynolds number for all cases under investigation, the dynamic pressure variations have a similar trend. Also, it can be seen that as the NTT increases that leads to generating lower dynamic pressure variations close to the tape turn surfaces. The possible reason for that is due to the formation of more swirl flow, secondary flow and separation flow near and close these special regions in comparison with other regions. Additionally, these types of flow lead to

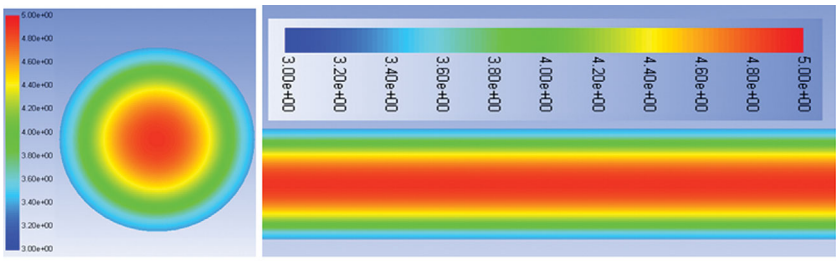

(a) Dynamic pressure variations contours in smooth pipe

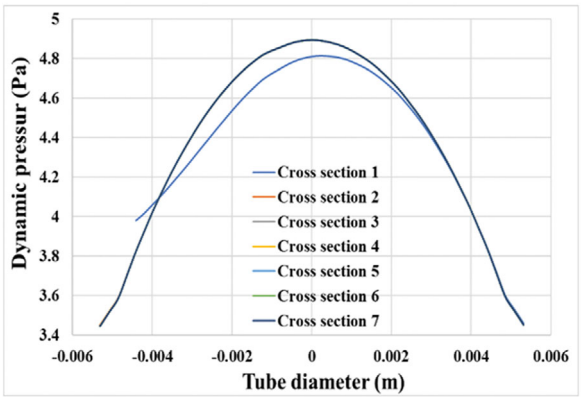

(b) Dynamic pressure profile in smooth pipe at different cross section areas

Fig. 11. (a) Dynamic pressure variations contours and (b) Dynamic pressure profile in smooth pipe.

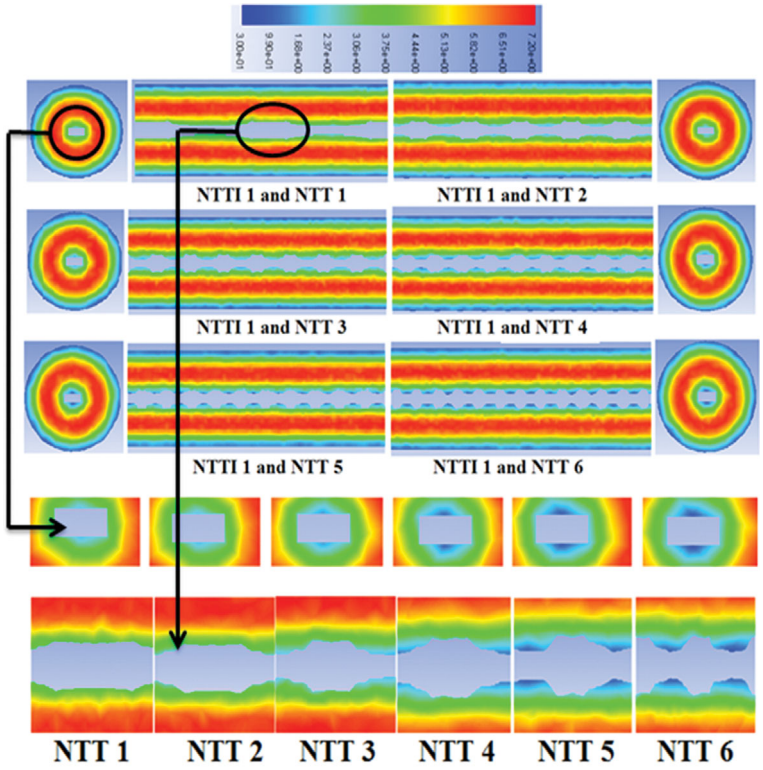

(a) Dynamic pressure variation contours

Fig. 12. (a) Dynamic pressure variation contours and (b) Dynamic pressure profile in twisted pipe under different NTT with one twisted tape insert.

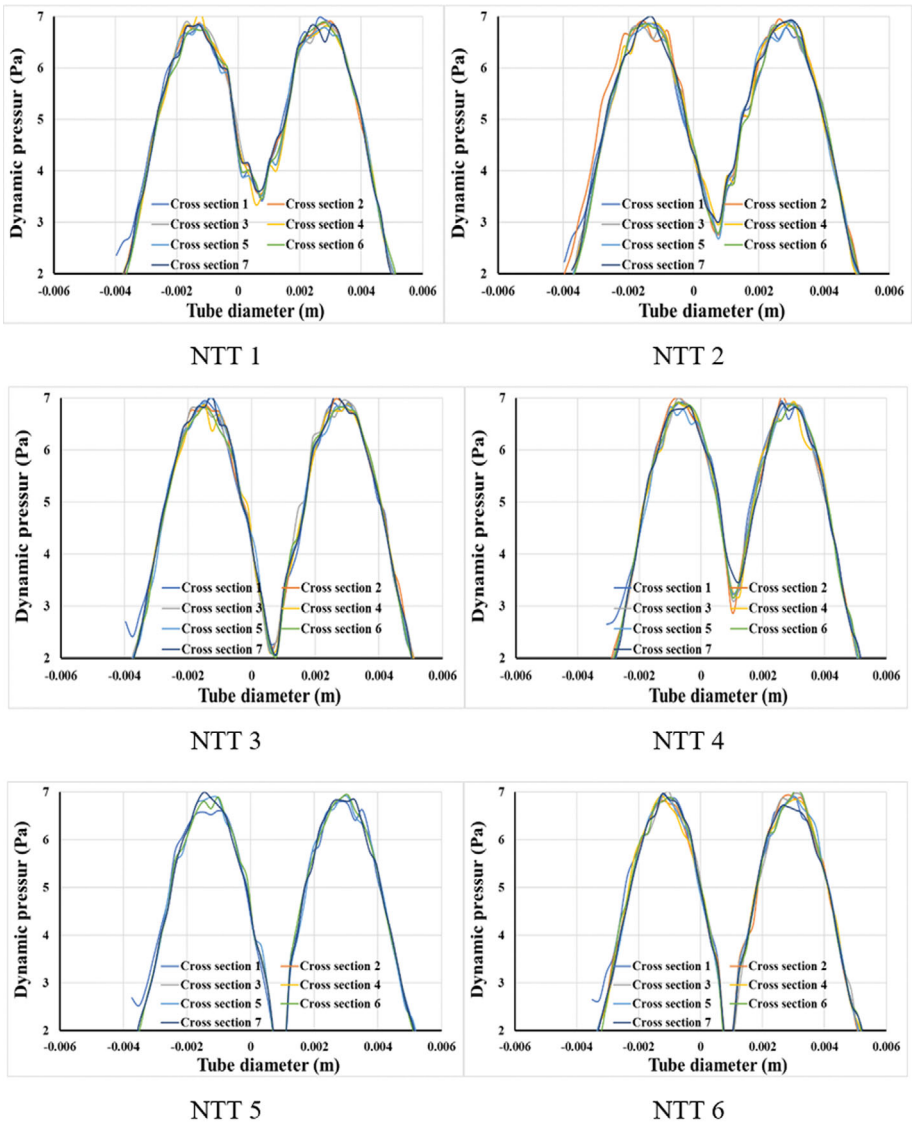

Fig. 12. Continued.

produce high fluid mixing with more components of tangential velocity.

Fig. 12(b) depicts the profile of dynamic pressure of water flow within the circular pipe with TTNI 1 at different NTT under different cross section areas. The quantitative results indicate that the dynamic pressure profile divided into two regions that occur because of the effect of twisted tape insert inside a pipe. Moreover, it can be observed that the maximum dynamic pressure takes place at the center distance between the twisted tape and outlet pipe diameter for both parts in the pipe. The reason behind that is due to the region having high velocity magnitude. Furthermore, the results show that the overall behavior for all cases has the same trend.

Figs. 13(a) and 14(a) depict dynamic pressure variation contours within the circular pipe with TTNI 3 and TTNI 5 at different NTT. It can be seen that the dynamic pressure changes as the NTT changes, and the maximum value of the dynamic pressure takes place at low NTT, especially at NTT 1 and NTT 1.

Figs. 13(b) and 14(b) depict the dynamic pressure curve profiles. According to these figures, it can be obviously observed that as the NTTI increases from three to five that leads to the flow in the pipe becoming more turbulent and the dynamic pressure profile is not uniform for all cases under investigation.

According to the above figure it was noted that when NTTI increases to five that leads to the dynamic pressure variations being greaer and more turbulent, especially between each twisted tape. This turbulent flow can cause more vortices in the flow and secondary flow.

Fig. 15(a) demonstrates the velocity magnitude variation and velocity profile in a pipe without twisted tape insert. It can be seen that higher velocity value takes place at the pipe center. Also, the minimum value reaches to outlet pipe area, due to the water flow in the pipe following classical hydromechanics behavior. Fig. 15(b)

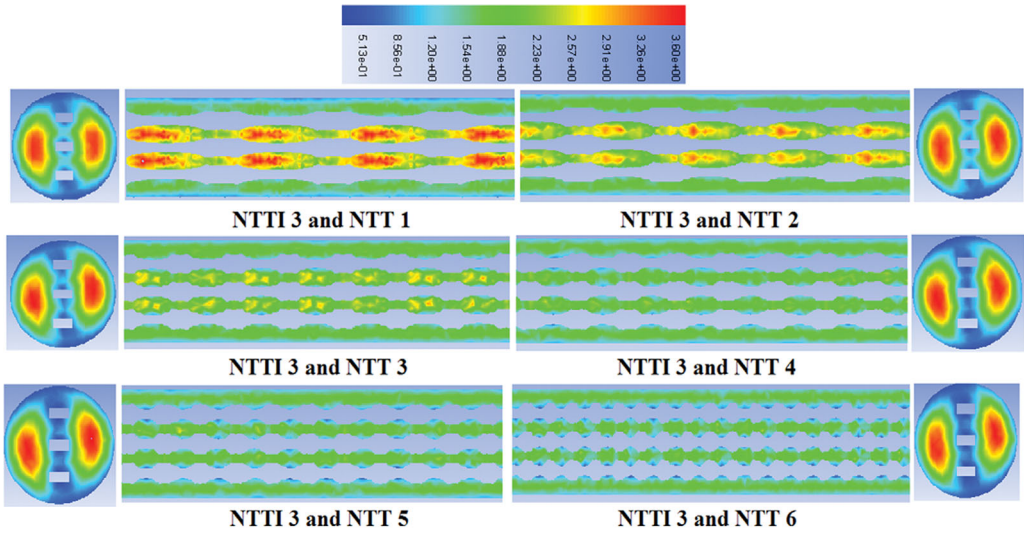

(a) Dynamic pressure variations contours

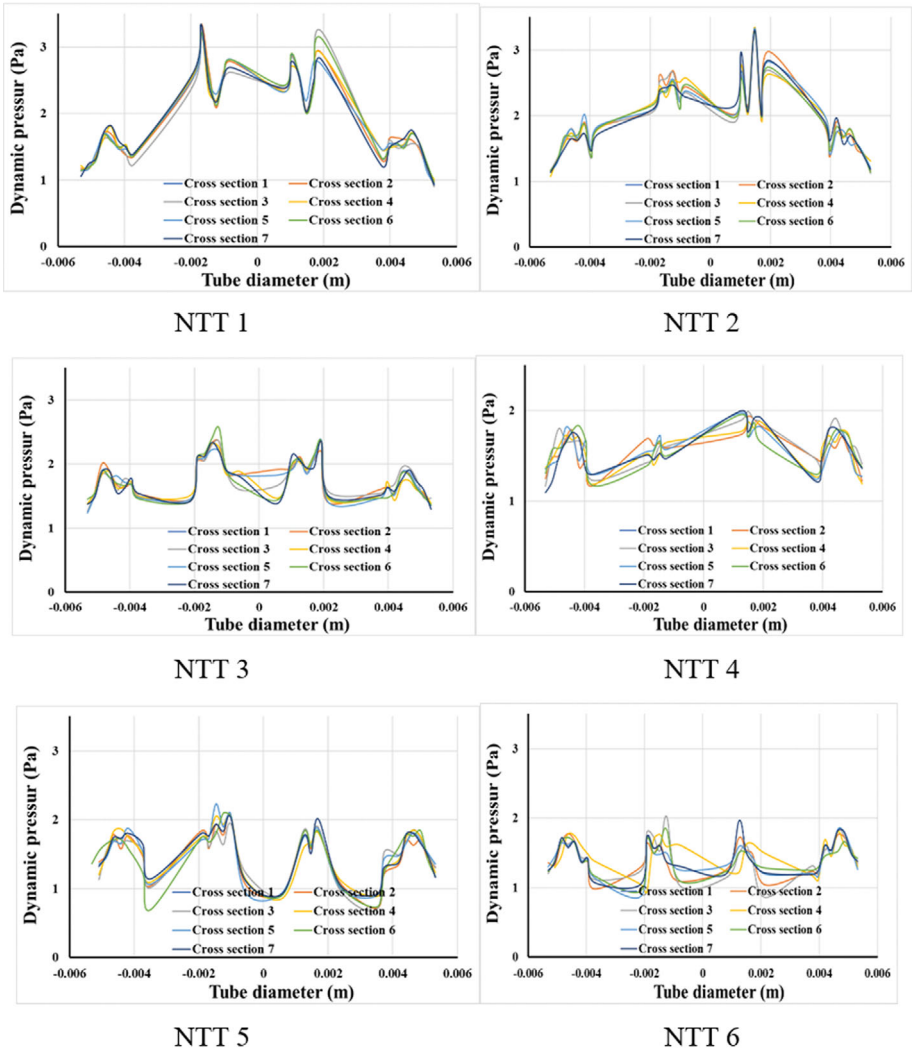

(b)

Fig. 13. (a) Dynamic pressure variation contours and (b) Dynamic pressure profile in twisted pipe under different NTT with three twisted tape inserts.

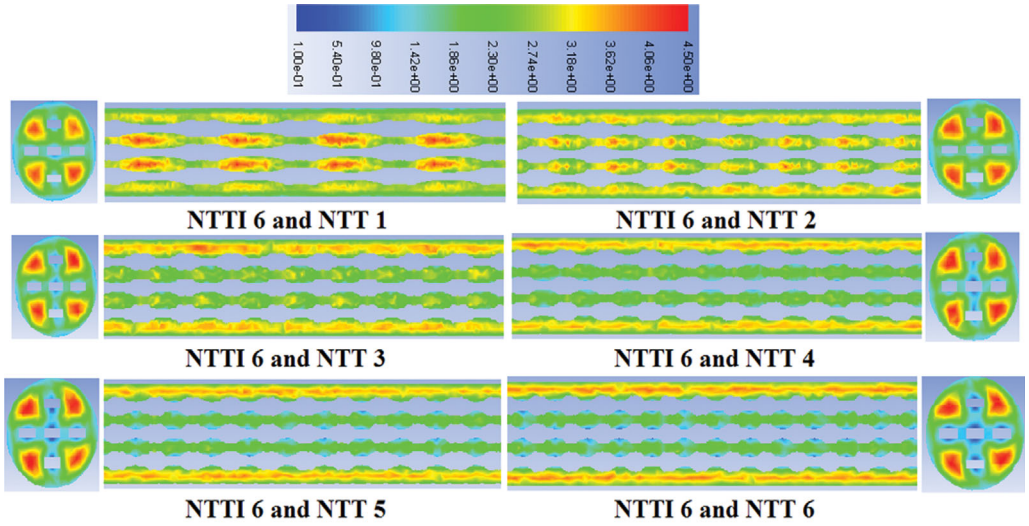

(a) Dynamic pressure variations contours

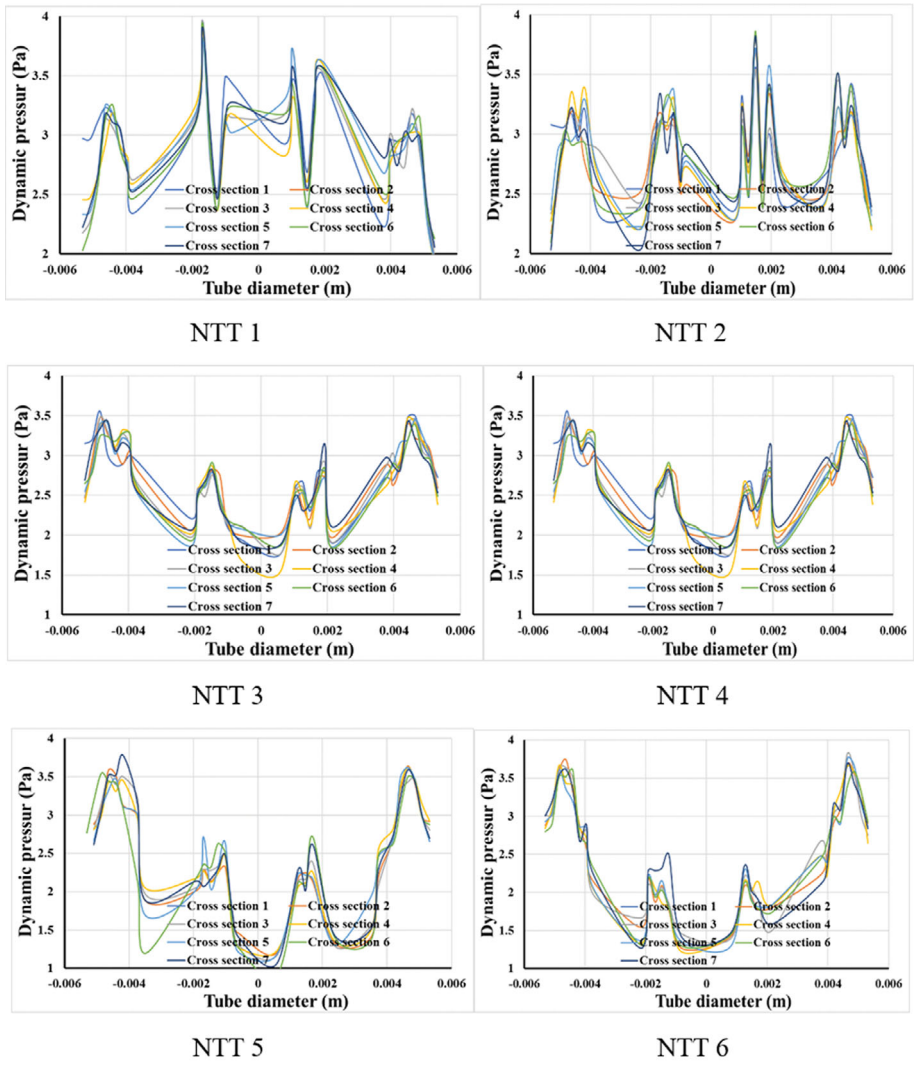

(b)

Fig. 14. (a) Dynamic pressure variation contours and (b) Dynamic pressure profile in twisted pipe under different NTT with five twisted tape inserts.

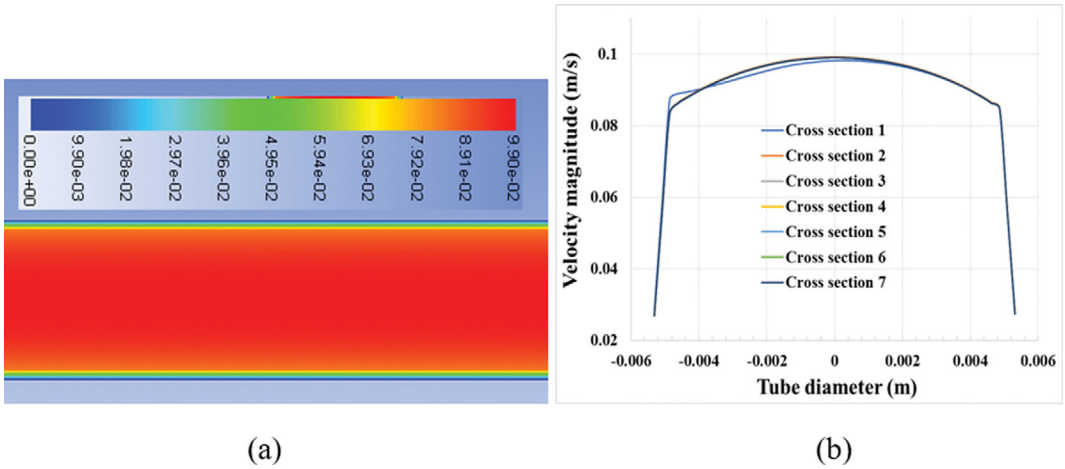

Fig. 15. (a) Velocity magnitude variationscontours in smooth pipe and (b) profile of velocity magnitude with various sections in pipe.

shows the velocity magnitude profile at various cross sections. It can be noticed that the velocity profile curves are very smooth; the higher velocity value occurs near the pipe center and it reduces when it reaches the outlet pipe.

In this part, the impact of inserts of twisted tape on the flow field is demonstrated. Fig. 16 depicts the velocity magnitude for the various configurations of twisted tape with various NTTs. As noticed, the existence of the twisted tapes inside the pipe can produce more

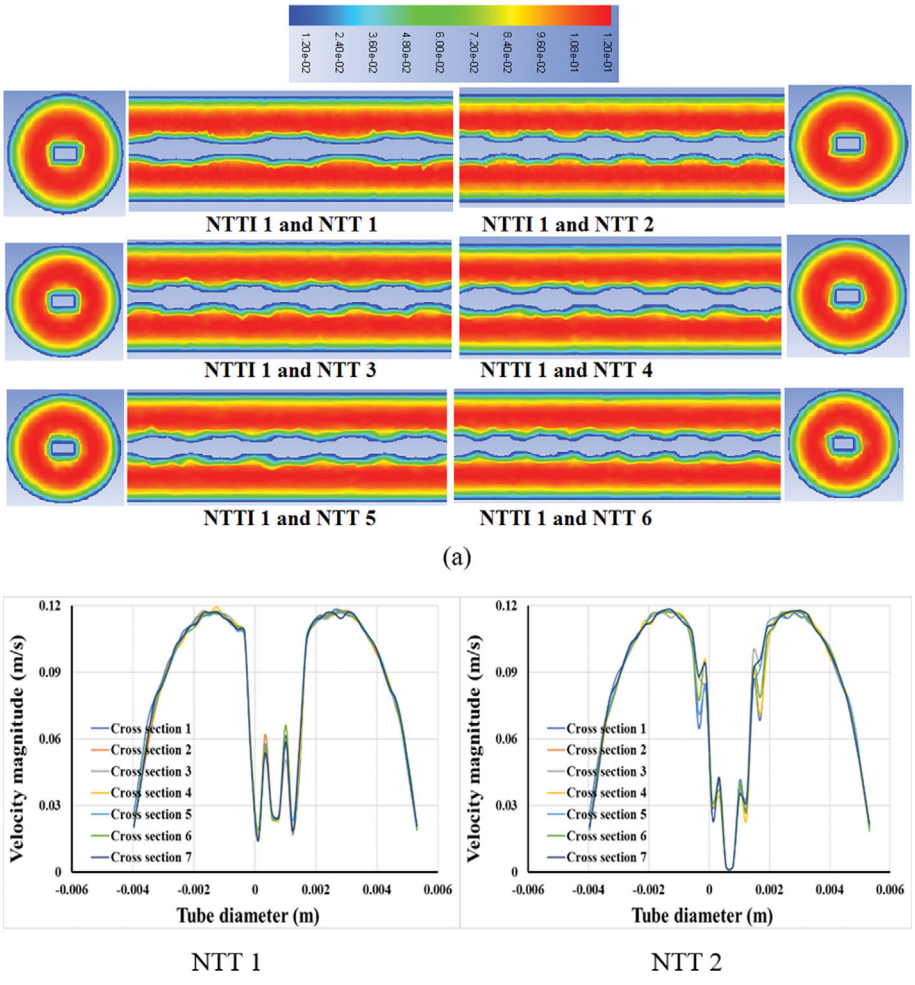

Fig. 16. (a) Velocity magnitude variation contours and (b) Velocity profile in twisted pipe under different NTT with one twisted tape inserts.

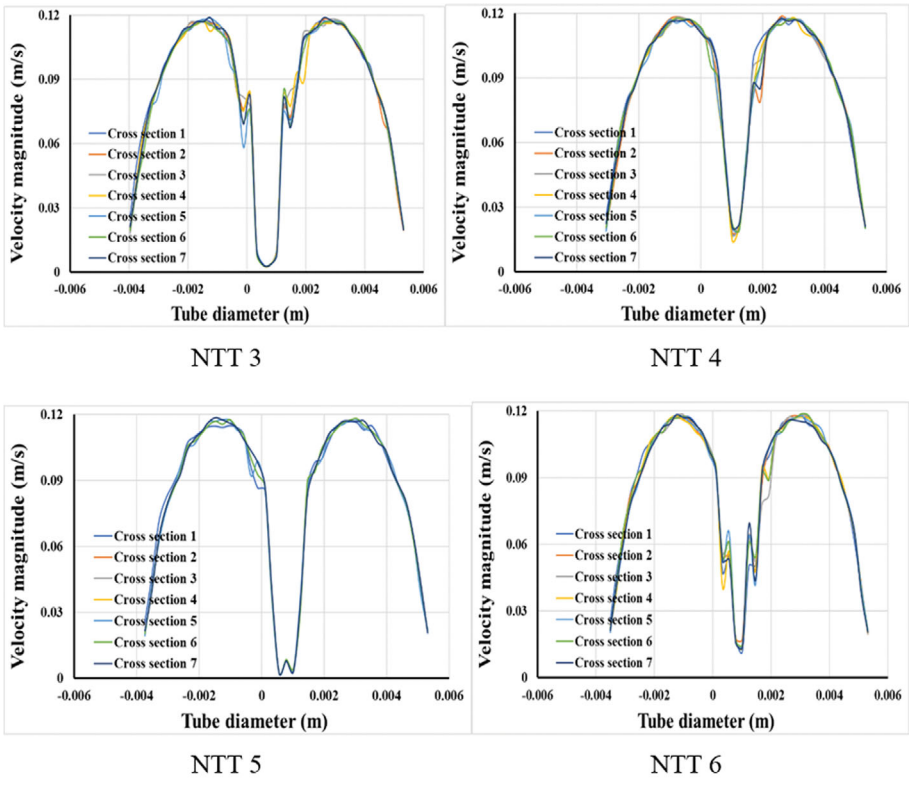

(b)

Fig. 16. Continued.

vortex motion (swirl flows), which leads to cause formation of different radial velocities. However, the creation of swirl flows is approximately different for each NTT. Based on this figure, the existence of the twisted tapes at the core of the pipe can cause the same flow revolution around every twisted tape, and hence divergent swirl flows take place at this region. Moreover, the swirl flows produced by the shape of the twisted tape can lead to be comprised of two different rotating flows at the upper and bottom of the twisted tape, hence causing development of converged swirl flows near and close the pipe center. In addition, more secondary flow can be impinged due to more intense twisted tapes.

Figs. 17(a) and 18(a) show the velocity magnitude at different

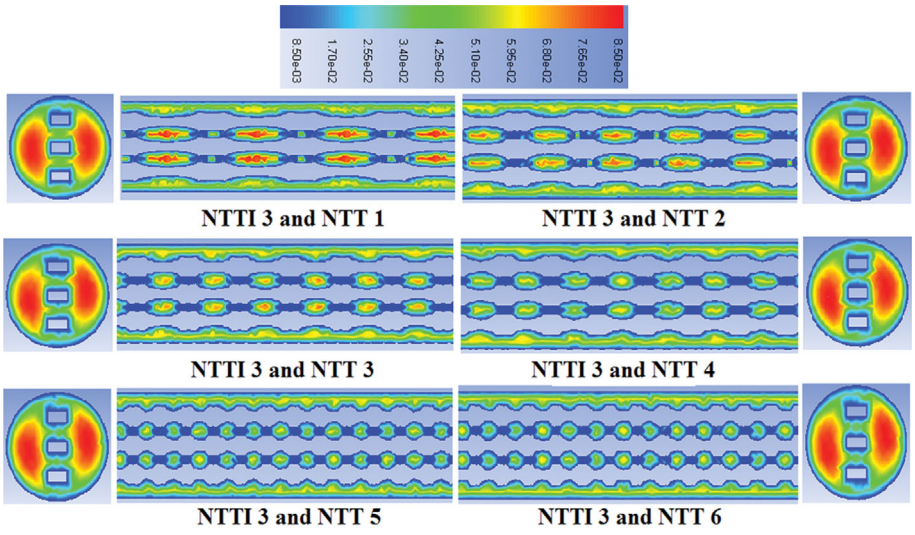

(a)

Fig. 17. (a) Velocity magnitude variation contours and (b) Velocity profile in twisted pipe under different NTT with three twisted tape inserts.

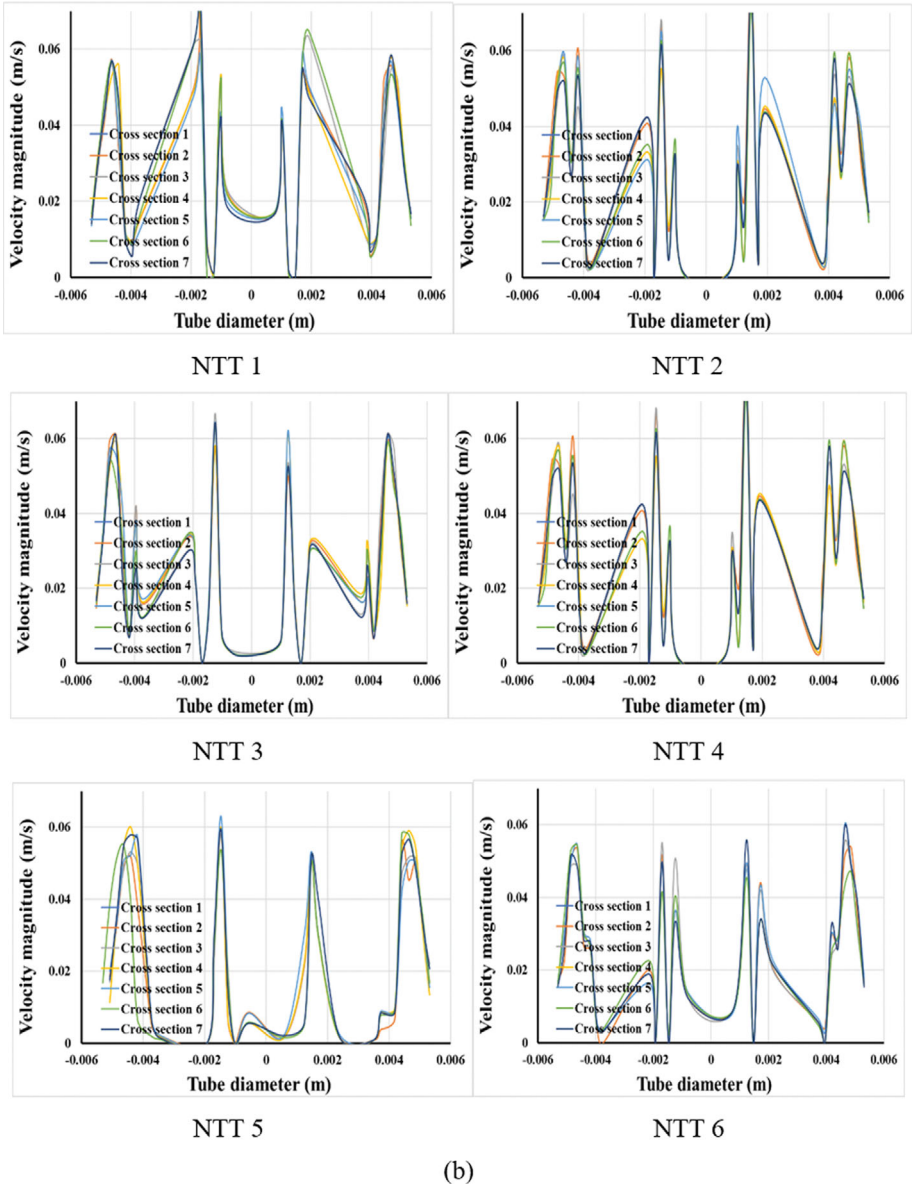

Fig. 17. Continued.

twisted tape inserts, including NTTI=3 and NTTI=5. From these figures, it can be observed that when the flows through the inserts along the pipe the water flow become more turbulent, that occurs due to twisted tape insert compelling curvature. Also, at different cross section can be noticed that more turbulence takes pace close and between each twisted tape. Moreover, that leads to producing the swirl and then vortex flow motion within a tube that can enhance and improve heat transfer performance.

According to the Fig. 17(b) it can be clearly observed that the profile of velocity in a pipe using the tape inserting under various NTT with three twisted tape inserts becomes more non-uniform at different NTTs, which can enhance the rate of heat transfer. With regard to this figure, it can be seen that the higher velocity takes place at the center between the twisted tapes. Based on the above results, it can be revealed that using twisted tape is more suitable to obtain higher rate of heat transfer.

Based on the below velocity magnitude profile, it can be seen that at different cross sections and NTTs due to the twisted tape curvature, that leads to generating more rotation flow in the pipe. Moreover, this rotation flow can produce more tangential direction and more fluid disturbance and hence that leads to generate whirling motion.

Fig. 19(a), (b) and (c) represent the change in value of Nu number, f and thermal performance evaluation factor (PEF) with NTT under various range of Re numbers. It is distinguished that as Re rises the value of Nu also increases, as well as when the NTT configuration geometrical parameters increase, that leads to the value of Nu increasing. Furthermore, the value of friction factor decreases as the NTT configuration increases due to increase of the flow resistance in flow direction leading to increase the pressure drop, and that agrees with previous works [27-29]. Also, the PEF factor decreases as the Re increases and value of the PEF is more than 1.6

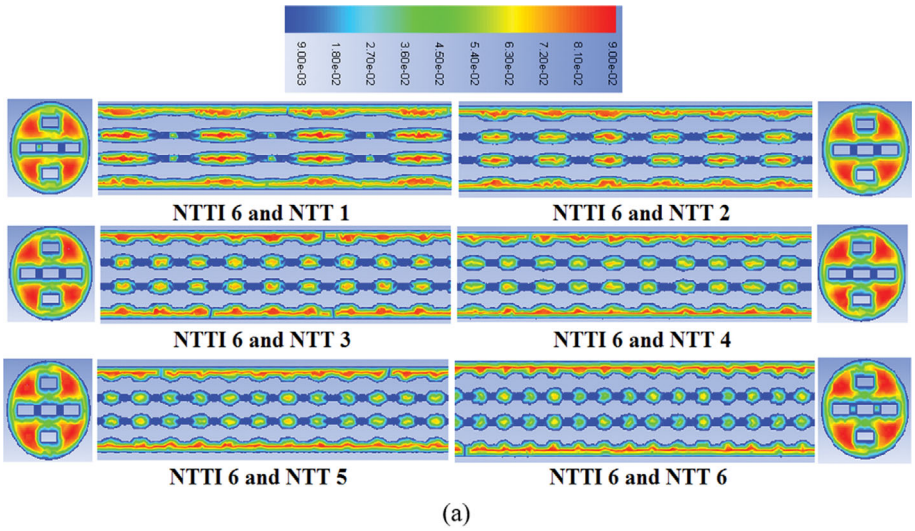

(a)

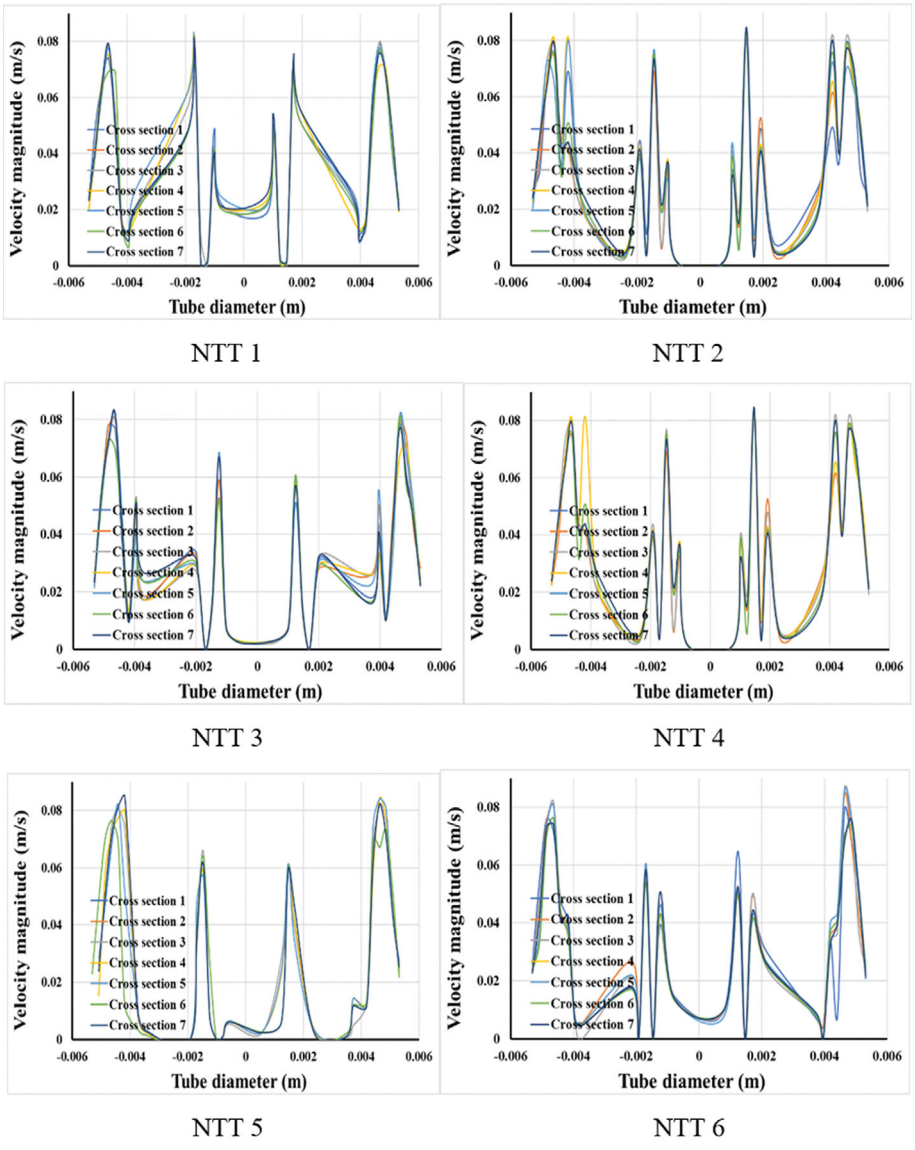

(b)

Fig. 18. (a) Velocity magnitude variation contours and (b) Vorticity profile in twisted pipe under different NTT with five twisted tape inserts.

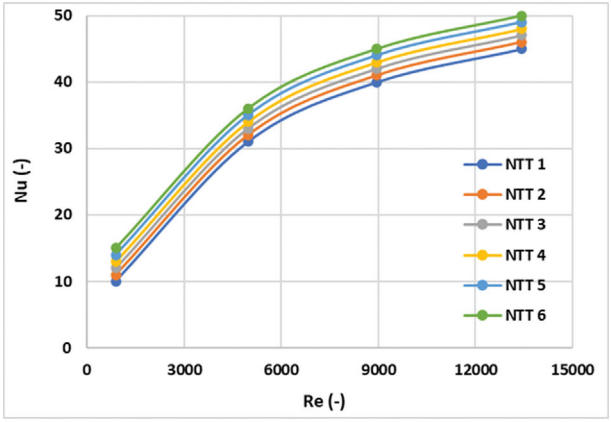

(a)

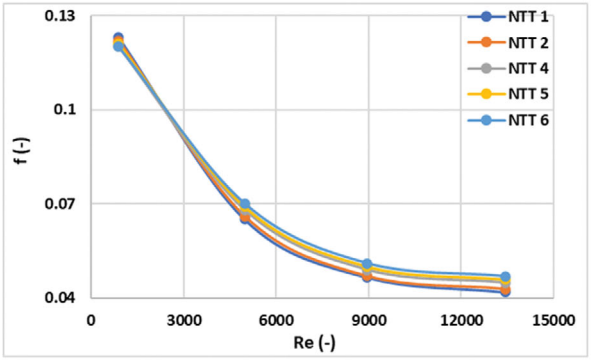

(b)

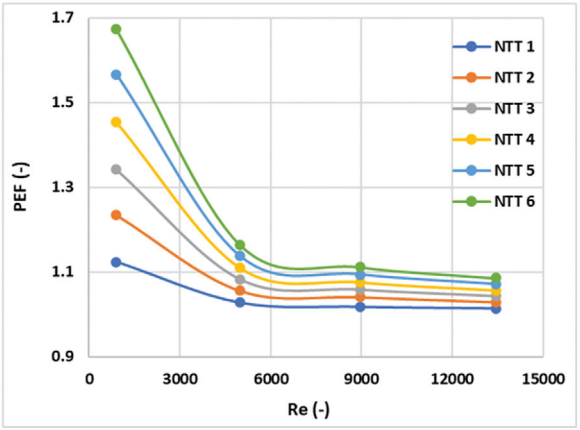

(c)

Fig. 19. (a) Nu number (Nu), (b) friction factor (f) and (c) PEF at different cross sections with one twisted tape insert.

for NTT6 configuration.

CONCLUSION

Various cases of using twisted tape inserts were analyzed in order to discuss the influences of NTTI and NTT on the thermal behavior, pressure drop and flow field on heat exchanger pipes by using numerical technique. Different conclusions can be found as follows: The comparison between the numerical and experimental results indicates that a good agreement the average deviation results between them for heat transfer was around 7%. Static pressure field in a smooth pipe gradually decreases as the length of pipe increases. A high-pressure region takes place at an inlet pipe. Also, the minimum value of pressure occurs near the outlet pipe. Pressure in twisted around region was more than the normal pipe because the twisted tape insert inside a pipe can cause more fluid resistance. The NTTI has high effect on the pressure difference. Moreover, the results have shown that NTT has little effect on the value of pressure difference. When the NTT increases in the twisted pipe that leads to generate lower dynamic pressure variations close to the tape turn surfaces. The maximum dynamic pressure takes place at the center distance between the twisted tape and outlet pipe diameter for both parts in the pipe. Existence of the twisted tapes inside the pipe can produce more vortex motion (swirl flows) that leads to cause formation of different radial velocities. The swirl flows produced by shape of twisted tape can lead to comprise two different rotating flows at the upper and bottom of the twisted tape and hence cause development the converged swirl flows near and closed the pipe center. The pattern of water flow within a tube with inserting of twisted tape is mainly not uniform and irregular and differs by alteration of the twisted tape longitudinal location. Thermal performance increases due to inserting the twisted insert tape in a pipe, that means the twisted insert tape has a good positive effect on the thermal system performance. The results indicate that the temperature difference increases to 38.1%, 46.11% and 50.52% with increasing the NTTI from 1 to 5, respectively, as compared to the temperature difference in a smooth pipe. The PEF factor decreases as the Re increases and the value of the PEF is more than 1.6 for NTT6 configuration.

ACKNOWLEDGEMENTS

The author in this existing numerical work wants to thank the Mustansiriyah University (www.uomustansiriyah.edu.iq) in Baghdad - Iraq for its support.

AUTHOR ORCID ID

Asst. Prof. Dr. Ahmed Ramadhan Al-Obaidi
https://orcid.org/0000-0003-3819-7008

LIST OF NOMENCLATURE

C_p : specific water heat [J/kg·K]
Di : inlet diameter of pipe [m]
f : friction factor [-]
fo : Smooth pipe friction factor [-]
Q : rate of heat transfer [W]
k : thermal water conductivity [W/m·K]
L : all length of pipe [m]
Nu : Nusselt Number in smooth pipe [-]
Nuo : Pipe with twisted tape Nusselt Number [-]
P : pressure in pipe [Pa]
Re : Reynolds Number [-]
T : water temperature [°C]

ΔT : temperature difference [°C]
Pr : Prandtl number [-]
U : velocity flow [m/s]
Ui. Uj, Uk : direction of velocity flow in X, Y and Z [m/s]
μ : dynamic water viscosity [N·s/m^2]
ρ : water density [kg/m^3]

REFERENCES

1. S. Eiamsa-ard, K. Wongcharee and P. Eiamsa-Ard, *Appl. Therm. Eng.*, **30**(4), 310 (2010).
2. A. R. Al-Obaidi, *J. Energy Storage*, **26**, 101012 (2019).
3. S. Eiamsa-ard, C. Thianpong, P. Eiamsa-Ard and P. Promvonge, *Int. Commun. Heat Mass Transfer*, **36**(4), 365 (2009).
4. A. R. Al-Obaidi and A. Sharif, *J. Therm. Anal. Calorim.*, **143**(5), 3533 (2020).
5. W. He, D. Toghraie, A. Lotfipour, F. Pourfattah, A. Karimipour and M. Afrand, *Int. Commun. Heat Mass Transfer*, **110**, 104440 (2020).
6. A. R. Al-Obaidi, *Heat Transfer*, **49**(8), 4153 (2020).
7. M. Ghalambaz, R. Arasteh, H. Ali, H. M. Talebizadehsardari and W. Yaïci, *Symmetry*, **12**(10), 1652 (2020).
8. F. Pourfattah, M. Sabzpooshani, D. Toghraie and A. Asadi, *J. Therm. Anal. Calorim.*, **144**(1), 189 (2021).
9. T. Dagdevir and V. Ozceyhan, *Int. J. Therm. Sci.*, **159**, 106564 (2021).
10. S. D. Salman, A. A. H Kadhum, M. S. Takriff and A. Mohamad, In *IOP Conference Series: Mater. Sci. Eng.*, **50**, 012034 (2013).
11. D. Erdemir, V. Ozceyhan and N. Altuntop, *World Sci. Eng. Acad. Soc., WSEAS*, **1**, 167 (2013).
12. K. P. V. Krishna varma, P. S. Kishore and T. Tirupathi, SSRG Int. J. of Mechanical Engineering (SSRG-IJME) - Special Issue (2017).
13. N. Mashoofi, S. Pourahmad and S. M. Pesteei, *Case Stud. Therm. Eng.*, **10**, 161 (2017).
14. R. Hosseinnejad, M. Hosseini and M. Farhadi, *J. Therm. Anal. Calorim.*, **135**(3), 1863 (2019).
15. A. Saravanan and S. Jaisankar, *Int. J. Therm. Sci.*, **140**, 59 (2019).
16. S. Alzahrani and S. Usman, *Therm. Sci. Eng. Prog.*, **11**, 325 (2019).
17. D. Xi, J. Liu, W. Li, Z. Li, Z. Jin, L Zhong and L. Li, *IEEE Trans. Appl. Superconductivity*, **29**(2), 1 (2019).
18. M. E. Nakhchi and J. A. Esfahani, *J. Heat Transfer*, **141**(4), 041902 (2019).
19. Y. Liang, P. Liu, N. Zheng, F. Shan, Z. Liu and W. Liu, *Appl. Therm. Eng.*, **148**, 557 (2019).
20. Y. Hong, J. Du and S. Wang, *Int. J. Heat Mass Transfer*, **115**, 551 (2017).
21. S. Kumar, P. Dinesha, A. Narayanan and R. Nanda, *Heat Transf.—Asian Res.*, **48**(7), 3399 (2019).
22. N. Piriyarungrod, M. Kumar, C. Thianpong, M. Pimsarn, V. Chuwattanakul and S. Eiamsa-Ard, *Appl. Therm. Eng.*, **136**, 516 (2018).
23. H. Safikhani and F. Abbasi, *Adv. Powder Technol.*, **26**(6), 1609 (2015).
24. M. Ghalambaz, H. Arasteh, R. Mashayekhi, A. Keshmiri, P. Talebizadehsardari and W. Yaïci, *Nanomaterials*, **10**(9), 1656 (2020).
25. H. Arasteh, A. Rahbari, R. Mashayekhi, A. Keshmiri, R. B. Mahani and P. Talebizadehsardari, *Int. J. Therm. Sci.*, **170**, 106966 (2021).
26. M. Ghalambaz, H. I. Mohammed, J. M. Mahdi, A. H. Eisapour, O. Younis, A. Ghosh and W. Yaïci, *Energies*, **14**(6), 1619 (2021).
27. R. Mashayekhi, H. Arasteh, P. Talebizadehsardari, A. Kumar, M. Hangi and A. Rahbari, *Heat Transf. Eng.*, **43**(7), 608 (2022).
28. R. Mashayekhi, H. Arasteh, P. Talebizadehsardari, A. Kumar, M. Hangi and A. Rahbari, Heat *Transf. Eng.*, **43**(7), 608 (2022).
29. M. Ghalambaz, J. M. Mahdi, A. Shafaghat, A. H. Eisapour, O. Younis, P. Talebizadeh Sardari and W. Yaïci, *Sustainability*, **13**(5), 2685 (2021).
30. A. R. Miandoab, S. A. Bagherzadeh and A. H. M. Isfahani, *Eng. Anal. Boundary Elements*, **140**, 1 (2022).
31. A. Aghaie and A. A. Rabienataj Darzi, *Heat Transf. Asian Res.*, **48**(1), 233 (2019).
32. A. T. Wijayanta, B. Kristiawan and M. Aziz, *Energies*, **12**(2), 306 (2019).
33. A. W. Albanesi, K. D. Daish B. Dally and R. C. Chin, 2nd Australasian Fluid Mechanics Conference Adelaide, Australia (2018).
34. F. P. Incropera, D. P. DeWitt, T. L. Bergman and A. S. Lavine, *Fundamentals of heat and mass transfer*, sixth ed., John Wiley & Sons (2006).
35. Y. Hong, J. Du, Q. Li, T. Xu and W. Li, *Energy Convers. Manage.*, **185**, 271 (2019).